CHAPTER 2

Experimental Procedure

Chapter 2 deals with the methods used for sample synthesis and different experimental technique employed for its characterization.

2.1 Sample Synthesis:

In the present investigation, both pyrochlore and double perovskite compositions were synthesized by solid state reaction method. Later, all the prepared samples were characterized by measuring their structural, magnetic and transport properties.

2.1.1 Solid State Reaction Route:

For oxide polycrystalline solid samples, conventional solid state reaction method is the widely used sample preparation method. For this route, the stoichiometric mixtures of different starting samples are used as precursors. Solid state method needs high temperature to heat the sample i.e. about 1000^0 C to 1500^0 C, The room temperature is not suitable for this method as solids do not react together at room temperature over normal time scales. This nature may be happens due to their different melting points. Moreover, an appropriate cooling rate is also required for the same. The other factors like feasibility, surface area of solids, structural properties of reactants, activation energy and the change in thermodynamic free energy are also required attention. The general schematic flow chart which shows the different steps under the reaction kinetics used for synthesis of the samples by solid state route is shown in fig. 2.1.

In our research work, we have taken the highly pure oxides of elements as precursors for sample preparation. The properly weighed stoichiometric ratios of oxides are mixed in an agate mortar for 2 hours. Then, the mixed powders were calcined in a muffle furnace at

different temperatures. After heating, the calcined powders were grounded and characterized by X-ray powder diffraction (XRD) to check the formed phase. After that, calcined powder is pressed into pellets by the hydraulic press under 5k Bar pressure. For sintering process, the pellets are kept in muffle furnace at suitable high temperatures.

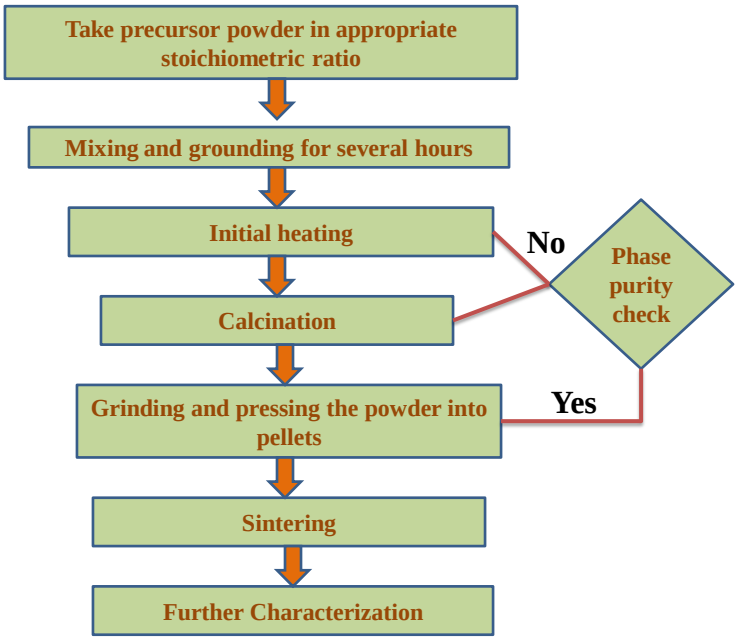

Figure 2.1: Flow chart showing the steps of solid state reaction method.

The appropriate phase formations of sintered samples were again verified by XRD pattern and then all other different material characterization techniques were adopted for their structural, magnetic and transport property study.

2.2 Experimental characterization techniques and their working principles:

This part deals with the importance and working principle of different characterization techniques which we were used in our research work.

2.2.1 Characterization tools for structural property study:

2.2.1.1 X-Ray Diffraction (XRD) technique:

The diffraction process occurs when any electromagnetic radiation interact with the periodic structure of system. X-rays are very high energy electromagnetic wave with very short wavelength. Thus, bending of X-ray around the corner of an obstacle is called diffraction. To examine the structure of crystalline solids, X-ray diffraction (XRD) technique is widely used. Not only this most fundamental and non-destructive technique used for phase identification, but also provides the information of unit cell dimension of structure. X-ray pattern of sample is displayed by variation of angle (2θ) with measured intensity.

Basic Principle:

The X-ray diffraction is based on the Bragg's Law, discovered by Sir William H. Bragg and Sir W. Lawrence Bragg. Bragg's Law describes the relationship between the angles at which X-ray beam of particular wavelength diffracted from a crystalline lattice [145]. Bragg's law stated as

$$\mathbf{2dSin\theta = n\lambda} \qquad (2.1)$$

Where, d= Inter plane distance of atoms

n = Integer displaying the order of diffraction peak.

λ= wavelength of the incident X-rays

θ= Scattering angle or Bragg's law

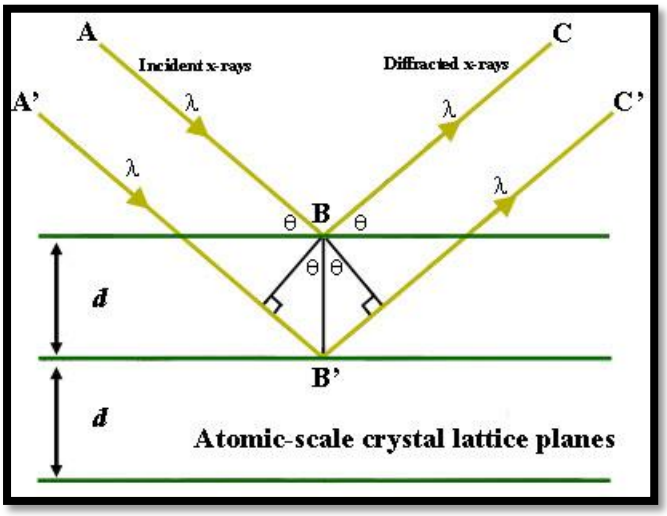

Figure. 2.2: Schematic diagram of Bragg's law

In this mechanism, cathode ray produced the X-ray beams and these beams are filtered to obtain monochromatic radiation, After than on collimate to concentrate, they fall on the surface of sample. A diffracted ray is obtained due to constructive interference between incident X-ray and sample. Finally, all diffracted rays are detected, processed and counted. The Rigaku-Miniflex II DESKTOP powder X-ray diffractometer has been used for phase identification of our samples which is shown in fig. 2.3. In this diffractometer, a monochromatic X-ray radiation of copper source (Cu-Kα = 1.5418 Å) at 30 kV and 15 mA was used.

Figure 2.3: Picture of Rigaku-MiniFlex-II DESKTOP powder X-ray diffractometer which we have used.

In order to obtain different parameters of crystal structure and to understand the cite symmetry variation, we have used Rietveld refinement. R. M. Rietveld has discovered this crystal's structure profile refinement method [146]. This method is the best fit method for the powder diffraction data of X-ray and neutron radiations. In Rietveld refinement, the laest square refinement is applied to obtain the structure factor of the material. The entire observed powder diffraction pattern along with entire calculated pattern of crystal structure is obtained by Rietveld refinement Model. Fullproof software has been used for Rietveld refinement of sample in present thesis.

2.2.1.2: Raman Spectroscopy:

In order to find out the vibrational, Rotational and low frequency modes of the sample, Raman spectroscopy have been employed. In Raman spectroscopy, the crystal structure of sample is acquired by the scattering of radiation. The credit of discovery of Raman spectroscopy has been given to Indian Physicist Raman and Krishnan. Prof. C.V. Raman got Nobel Prize for his "Raman Effect" theory. In 1928, they saw Raman Effect by using

sunlight as a source, their eye as detector and telescope as a collector. However, now- a-days, well equipped spectrometer has been used.

Basic Principle:

When an electromagnetic radiation scattered on a crystal or molecule, most of photons are scattered elastically. Thus, the energy (or wavelength) of both scattered photons and incident light are same. A very few part of light shows inelastic scattering. The elastic scattering is known as Rayleigh scattering, whereas, inelastic scattering is considered to Raman Effect. Because, in inelastic scattering, the frequency of scattered photons and incident light are differ. Hence, Raman spectra can be achieved by inelastic scattering of monochromatic radiation. In such condition, change in energy of photons may be increased (shifting up) or decreased (shifting down). This shift in energy of photons is known as Raman shift.

Selection Rule:

In electric field E, the molecular deformation i.e. change in the distortion of electron cloud of an atom or molecule is calculated by molecular polarizability (α).

$$\text{When} \quad \frac{\partial \alpha}{\partial Q} \neq 0 \qquad [\text{Q = normal co-ordinate}] \tag{2.2}$$

i.e. the Raman shift can be formed optically when the value of first derivative of polarizability with respect to normal coordinate becomes non zero. In this process, the molecules are starting to vibrate with the characteristics frequency $\gamma_m$due to molecular deformation. Thus, oscillating dipoles emit light of the frequencies of γ_0, γ_0-γ_m and γ_0+ γ_m , where γ_0 is the frequency of light emitted by monochromatic laser. As a result, Raman

Effect shows three type of scattering which depicts in fig. 2.4. The scattering corresponds to γ_0 is known as Rayleigh elastic scattering and the scattering corresponds to frequency γ_0-γ_m is called Stokes Raman Scattering, while the scattering corresponds to frequency γ_0+ γ_m is known as anti-stokes Raman Scattering. Generally, Raman Spectra has shown in wavelength (cm^{-1}). Hence, Raman shift ($\Delta\omega$) can be expressed in wave number as

$$\Delta\omega = \frac{1}{\lambda_0} - \frac{1}{\lambda_1} \tag{2.3}$$

Here λ_0 is excitation wavelength and λ_1 is Raman spectrum wavelength.

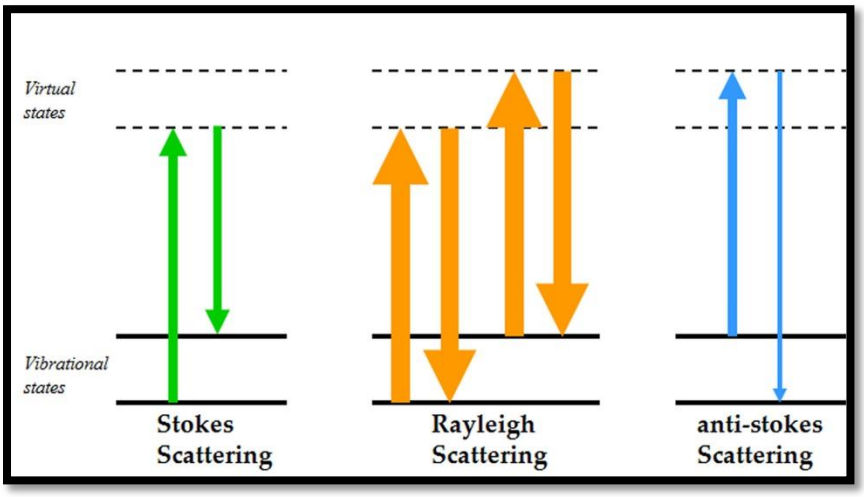

Figure 2.4: Energy level diagram of Rayleigh scattering and Raman Scattering

Fig. 2.5 shows the Renishaw Raman spectrometer in which we have recorded Raman spectra of our samples at different temperatures along with room temperature. In this spectroscope, a diode pumped solid state laser of 532 nm wavelength is used monochromatic radiation source.

Figure 2.5: Picture of Renishaw Micro Raman Spectrometer

This pumped source used 5 % of 100 mW power to avoid laser-induced heating in the compositions. The incident laser beam has to focus over a 50 x long-distance objective which is linked to Leica DM 2500 M microscopy. To focus on an objective, Laser beam has travelled a very short working distance. For dispersion, a grating of 2400 groves/mm is equipped and slit width of 50 micron is kept constant during whole experiment for maintaining constant phase. The scattered radiation is collected at back scattered position which is passed further through the filter. To eliminate the unwanted part of scattered radiation, filter has been used. Finally, the radiation is fed to the detector. Moreover, liquid nitrogen is added to this Raman spectrometer to measure temperature dependent Raman Spectra. The supplied 4.0 software spectrometer has been used in scanning, data collection and processing of our data.

2.2.1.3 Neutron Powder Diffraction (NPD) technique:

Elementary particle neutron which was discovered by James Chadwick in 1932 becomes an important part in research area of condensed matter [147]. Scientist Brockhouse and Shull implemented the neutron scattering technique [148]. This NPD technique is renowned everywhere for describing the both atomic structure and magnetic spin structure of crystal. Actually, X-ray diffraction (XRD) and neutron diffraction both are used to determine the crystal structure. But at some point, NPD technique has some peculiar features to over X-ray diffraction like.

1. In XRD, photon is scattered by electron cloud whereas, in NPD, neutron is scattered by nucleus of atom. So, neutrons are relatively scattered more powerfully from 'light' atoms like Hydrogen (H) and Oxygen (O). Hence, NPD is more preferable in case of heavier elements.
2. In XRD, scattering cross section area of element varies as Z^2 (Z = atomic number), whereas there is no such relation found in cross section area and atomic number in NPD. This haphazard variation between the neutron scattering cross section of elements like manganese (Mn) and Iron (Fe) helps from them to be different from each other [149].
3. Neutrons have no form factor. So, they act as a point scatterer. Thus, range of data in reciprocal space which achieved from diffraction is increased, whereas, XRD has form factor which generates from size of electron cloud surrounding the nucleus.

Basic Principle:

The basic principle of all diffraction experiments is Bragg's law. This experiment has carried out by two methods. In first method, the position of detector is not fixed, it can be varies in a wide range of angles. When a sample is targeted by a monochromatic neutron

beam (whose wavelength is λ_0), moveable detector measures different inter-planar d spacing d_{hkl} (hkl= miller indices). Bragg's law for this method can be stated as

$$\boldsymbol{\lambda_0 = 2\, d_{hkl} \mathrm{Sin}\theta_{hkl}} \quad (2.4)$$

The diffractometer which are based on this moveable detector method called constant wavelength or steady state diffractometer. In second method, instead of wavelength, position of detector is fixed. It kept fixed at angle θ_0. Variable wavelength is provided by a white spectrum in this method.

The interaction of neutron with matter is followed by two ways. In first way, neutron interacts with the nuclei of crystal. While, in the second way, there is the magnetic interaction between the neutron spins and the atomic spins. Thus, first interaction is known as nuclear scattering, whereas second one is known as magnetic interaction. Due to interaction between magnetic spins and atomic spins, NPD gives the information of magnetic spin structure of a sample. Moreover, direction of alignment of moments decides the amplitude of scattering. Therefore, NPD is used to display the arrangements of atomic magnetic spin moment in a magnetic sample. Hence, NPD technique is quiet useful in magnetism.

The properties of neutrons are summarized as

a) Charge = 0 (neutral)

b) Mass = 1.674 x 10^{-27} Kg

c) Wavelength (λ)= $\frac{0.0286}{\sqrt{E}}$

d) Spin = ½

e) Magnetic dipole moment (μ_N) = -1.913

f) Life time = 881.5 $\pm$1.5 seconds ($\approx$15 minutes)

g) Velocity = 2200 m/s for thermal neutrons

We have collected all NPD data from PD2 (Powder Diffractometer-2) neutron powder diffractometer (λ =1.2443A°) at the Dhruva reactor in Bhabha Atomic Research Centre, Mumbai, India. The pictorial view of diferectometer is shown in fig. 2.6.

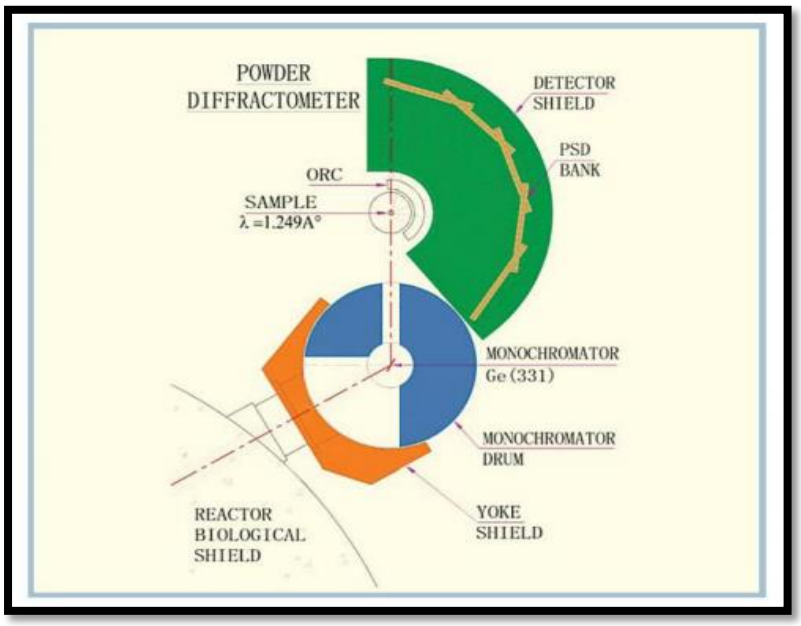

Figure 2.6: Shows the Setup of PD-2 (Powder Diffractometer-2) located at Bhabha Atomic Research, Mumbai, India.

2.2.1.4. X-ray Photoemission Spectroscopy (XPS) technique:

The true identification of oxidation state, elemental composition and ligand co-ordination is necessary for chemical and physical properties of samples. In order to identify these, X – ray photoemission spectroscopy (XPS) is extensively employed technique. This tool is also commonly known as photoelectron spectroscopy for Chemical Analysis (ESCA). The XPS measures the electronic and chemical state of elements present within a sample [120]. XPS collects the surface near generated electrons as it is a surface sensitive technique.

Basic Principle:

XPS technique is based on the photoelectric effect which was explained by Einstein in 1905. The photoelectric effect can be seen in fig. 2.7 a. Under XPS measurement, sample required to keep in an ultrahigh vacuum (~ 10^{-10} torr). The sample is irradiated by monochromatic and low energy X-rays (~ 1.5 keV) source. The core level electrons are ejected from the surface of sample due to photoemission process. In XPS spectra, the energy generated from the ejection of core-electron is treated as a function of binding energy of electrons. Thus, XPS spectra are plotted as a function of binding energy of detected electron displayed on X –axis and number of detected electrons (sometimes per unit time) are shown on Y-axis. Fig. 2.7 b shows the schematic diagram of XPS. The various parts of XPS spectroscopy are listed as

a) X-ray source.
b) Hemispherical electron energy analyzer
c) Vacuum system.
d) Neutralizer or electron flood gun.
e) Ar-ion gun.
f) Multi-channel detector plates.
g) Electronic control units.
h) Sample stage or holder.
i) Computer.

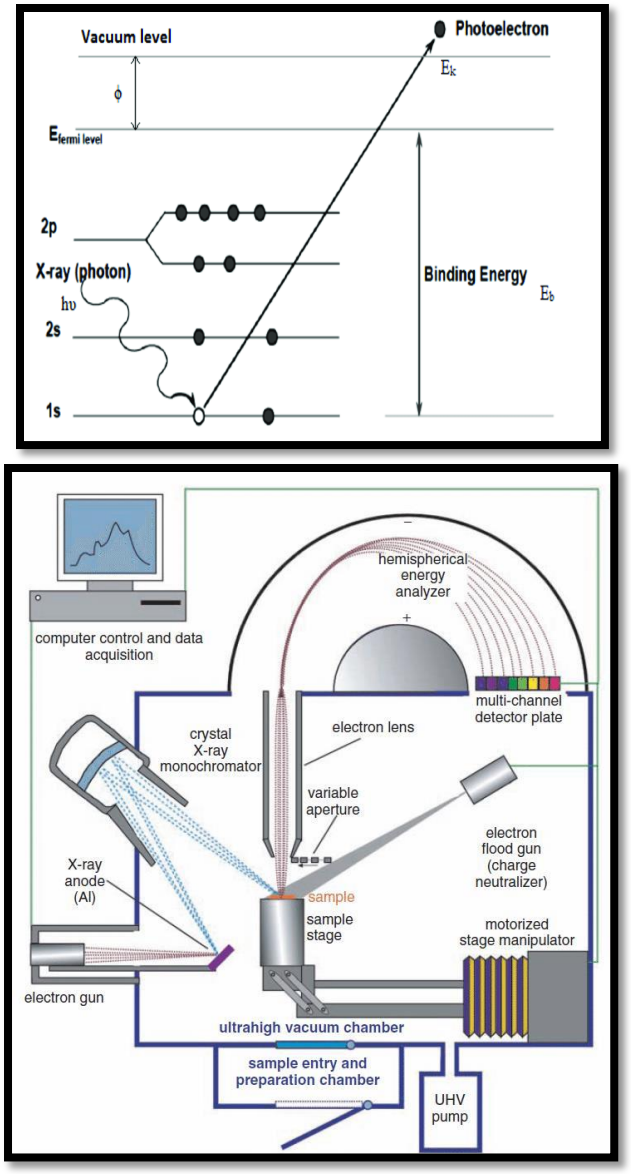

Figure 2.7 (a): Shows the photoelectric effect. **(b)** Depicts the schematic representation of XPS set up.

The energy of detected photoelectron can be determined by equation which is given by Ernest-Rutherford in 1914 is

$$E_{K.E.} = h\nu - (E_B + \phi) \quad (2.5)$$

Where, $E_{K.E.}$ is the kinetic energy of a electron which is measured by the spectrometer, $h\nu$ is the energy of incident X-ray photons , E_B is the binding energy of the electron, , and work

function of the spectrometer (not the material) is represented by ϕ. This equation can be understood by Fig. 2.7 (a).

2.2.1.5. X-ray Absorption Spectroscopy (XAS) technique:

The X –ray absorption technique is initiated by X-rays, like XPS technique. They both are belongs to X-ray spectroscopy. If transition between the levels occurs due to emission process then it is investigated by XPS technique. Therefore, XPS probes the decay process from the excited state, while, if the transitions are related to absorption, it is fitted for XAS technique. This records the data of ground state to excited state transition. Although both XAS and XPS help to determine the electronic and chemical states of elements in a molecule, XAS technique also determine the different spin states (low, intermediate and high) of elements.

Basic Principle:

In XAS, the incident X-ray photon is excited the core level electron to an unoccupied conduction level. Under this process, intra-atomic dipole selection rule ($\Delta l = \pm 1$) is followed. As XAS is an element specific tool, it records the element specific energy difference between core and conduction level. For this system, the energy lays between 0.1–100 keV or 16–16,022 J. The edge like K-, L- and M- edges defines the different excitation of levels i.e. from which level, the core electron is excited. It is a known fact that these levels have principle quantum number n = 1, 2, 3. Thus, K- edge refers to absorption of photoelectron from n = 1 (1s core) level, L- edge refers to absorption of photoelectron from n = 2 (2s or 2p core) level and M- edge refers to absorption of photoelectron from n = 3 (3d core) level. This mechanism can be easily understood by fig. 2.8.

The XAS spectrum of an atom is achieved by sharp rises in absorption which happened at particular X-ray photon energy. These sharp rises in absorption are called absorption edges. Moreover, circular polarization of X-ray in XAS tool provides the information about the spin orientation of elements and magnetic ordering present in material. The shape of absorption peak helps to determine the spin arrangement in the system.

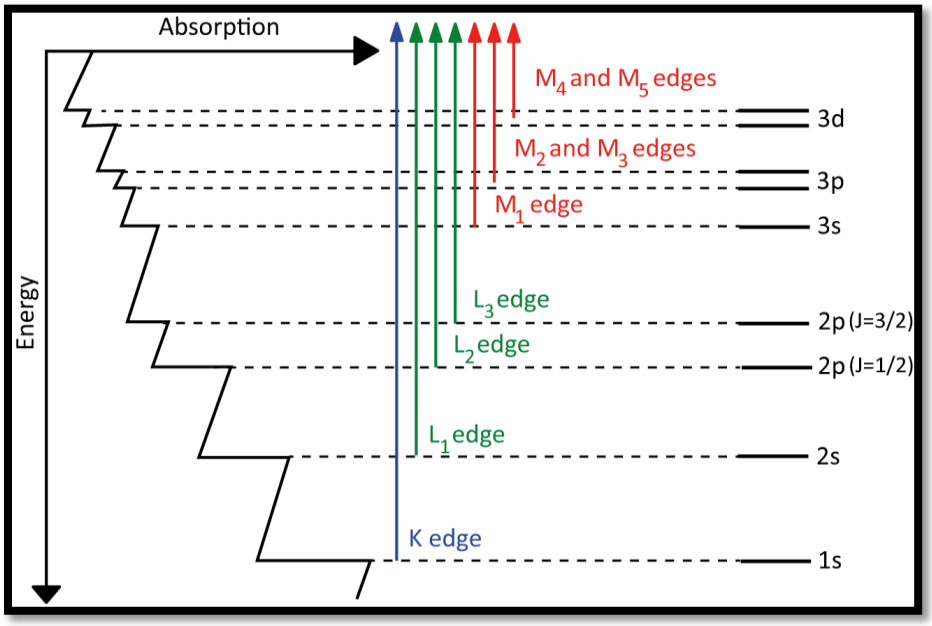

Figure 2.8: Transition between the core levels which rise to XAS edges.

Fig. 2.9 depicts the arrangement of different components of XAS beam line. In this arrangement, the function of mirror is to collimate and focus the beam, whereas, its size is defined by apertures and slits. A double crystal monochromator chooses the X-ray of minimal energy.

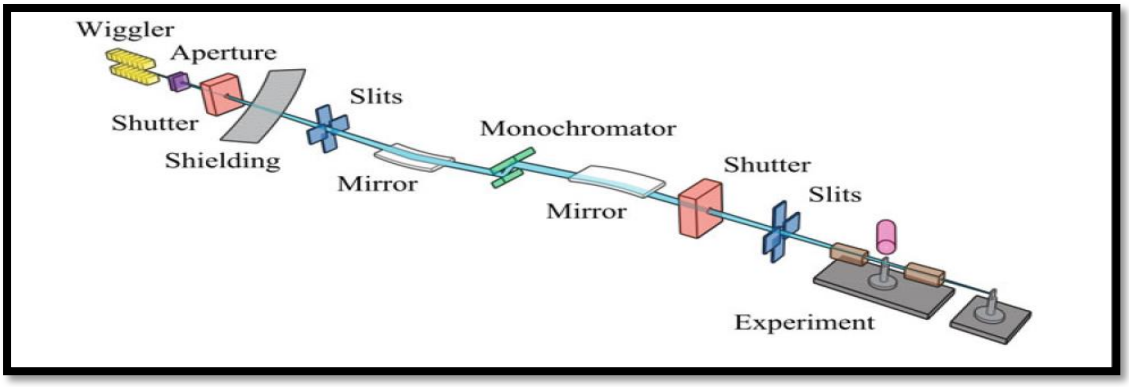

Figure 2.9: Block diagram of XAS beam line consists of various components.

In present thesis, we have performed our all XAS measurement at the BL14 beam line of Hiroshima Synchrotron Radiation Centre, Hiroshima University, Japan. A definite protocol which has taken to perform this XAS measurement is:

- Total electron yield (TEY) mode.
- Base pressure = 4×10^{-8} Pa
- Photon energy range of beam line = 400-1200 eV.

2.2.2 Characterization tools for magnetic property study:

2.2.2.1. Magnetic Property Measurement System (MPMS): SQUID-VSM

The superconducting quantum interference device (SQUID) is a powerful technique to measure very weak signal. SQUID is so impressive that it can able to measure the changes in the human body's electromagnetic energy field. This device measures such small magnetic field changes with immense precision.

Basic Principle:

Josephson effect and the flux quantization effect in superconducting rings rules the SQUID's function and it was firstly realized in 1963. In this system, two superconductors which are separated by thin insulating layer from two parallel Josephson junctions.

There are two types of SQUIDs based on superconducting rings which are interrupted at one point (Radio frequency SQUID) or two points (DC SQUID). The Quantum design MPMS measured the magnetic property through 3 possible modes.

1. DC scan mode. 2. AC susceptibility mode. 3. Vibrating sample magnetometer (VSM) mode.

VSM Mode:

According to Faraday's law of induction, 'an alternating magnetic field will induce the electric field and vice versa and VSM operation follow this law. In VSM, a material (pellet/powder) is kept under a uniform magnetic field. As a result, it gets magnetized and the magnetic domains of material are aligned in the direction of field. As the magnetic field increases, the magnetization is also increases. A magnetic field near the sample is also generated which is known s stray magnetic field. The stray magnetic field is induced by the magnetic dipole moment of sample. When the sample vibrates i.e. it is moved up and down direction, the stray magnetic field turns to be time dependent. This time varying changes in magnetic field is sensed by a set of pick-up coils and induces an electric field in these coils. Moreover, these pick up coils in SQUID are too sensitive to measure any minute changes. After that, induced current which is proportional to magnetization of sample, is amplified by

a lock-in amplifier and trans-impedance amplifier. The all various components are connected to computer. Controlling and monitoring software are used in magnetization measurement.

The spin dynamics of material is investigated by AC susceptibility mode, Therefore, it has to be mention that, at high frequency, AC susceptibility measurement gives two quantities (i) χ = magnitude of AC susceptibility (ii) $\emptyset$ = phase shift. Thus, AC susceptibility represent as complex quantity i.e.

$$\chi_{AC} = \chi' - i\chi''$$

Where, χ' is the in phase or real component and χ'' is the out phase or imaginary component. Both χ' and χ'' are sensitive to thermodynamic phase changes and display the phase transition.

MPMS has to follow a standard protocol to measure the magnetization of sample which is

- The strength of the constant magnetic field should not vary. It has to be fixed.
- The sample starts to oscillate.
- The signal which is received from the probe is converted into a value proportional to the magnetic moment of the sample.
- During this time, no data is taken.
- The constant magnetic field gets new value.
- Received signal from the probe is again converted to a new value of magnetization of sample.
- Magnitude of constant magnetic field changes in a given range and a graph of magnetization (M) Vs. magnetic field strength (H) is achieved.

All magnetic measurements of our samples are carried out through “Quantum Design MPMS 3 magnetometer” in 2 – 480 K temperature range which is shown in fig. 2.10.

Figure 2.10: Picture of Quantum Design MPMS 3 magnetometer located at CIF, IIT BHU, Varanasi.

2.2.3 Characterization tools for Dielectric study:

2.2.3.1 Dielectric Analysis:

The dielectric measurement is the versatile and very sensitive technique to measure the dielectric relaxation of an insulating and semiconducting sample. This tool is also characterized the other phenomenon like electrical conduction, dipolar ordering etc. The measured dielectric value of material is represented in the complex quantity form of electrical permittivity which contains both real and imaginary part i.e. $\boldsymbol{\varepsilon^* = \varepsilon' - i\varepsilon''}$**.** Here, ε' is real part and ε'' is imaginary part of electrical permittivity. Various physical parameters like frequency, temperature, pressure, electric or magnetic field can changes the value of electrical permittivity. From dielectric spectroscopy, dielectric relaxation (from ε^*), electrical relaxation (from M*) and impedance spectroscopy (from Z*) can be measure.

In present thesis, all dielectric measurement was carried out through a Keysight E4980A Precision LCR meter. This LCR meter is one of the most sensitive and more précised impedance analyzer.

Working Principle of the analyzer

In this analyzer, the sample is kept in between (middle) of two metal electrodes, forming a parallel plate type set up. For the measurement, a voltage generator energized a specimen by providing a harmonic signal V_s (f). Two phase sensitive voltammeters measure like current I_s(f) and phase shift across the specimen.

From Ohm's law, impedance Z* can be written as,

$$Z^* = \frac{Vs(f)}{Is(f)}$$

The observed impedance is connected with the capacitance of sample as

$$C^* = \frac{-i}{2\pi f Z^*}$$

From here, the dielectric permittivity can be calculated as

$$\varepsilon^* = \varepsilon' - \varepsilon'' = \frac{C^* d}{\varepsilon 0 A}$$

where, d is thickness of sample and A is the area of sample.

2.2.3.2 Magneto-Dielectric Analysis:

To correlate the magnetic spin dynamics with the electric field, we have performed magneto-dielectric (MD) measurement of our sample. The magneto-dielectric measurement set up shown in fig. 2.11.

Figure 2.11: Picture of magneto-dielectric measurement set up

This set up has various components,

- Vibrating sample magnetometer (VSM Lakeshore model 142A)
- a Keysight E4980A Precision LCR meter
- Two powerful magnet having strength upto 2 T.

The temperature dependent magneto-dielectric parameters like magneto-Capacitance (C) , magneto-dielectric loss (tanδ) are measured in the fixed 1.3 T magnetic field at 10 kHz frequency.